



This is a repository copy of *miR-200 promotes the mesenchymal to epithelial transition by suppressing multiple members of the Zeb2 and Snail1 transcriptional repressor complexes..*

White Rose Research Online URL for this paper:
<http://eprints.whiterose.ac.uk/93699/>

Version: Supplemental Material

Article:

Perdigao-Henriques, R., Petrocca, F., Altschuler, G. et al. (5 more authors) (2015) miR-200 promotes the mesenchymal to epithelial transition by suppressing multiple members of the Zeb2 and Snail1 transcriptional repressor complexes. *Oncogene*, 35. pp. 158-172. ISSN 0950-9232

<https://doi.org/10.1038/onc.2015.69>

Reuse

Unless indicated otherwise, fulltext items are protected by copyright with all rights reserved. The copyright exception in section 29 of the Copyright, Designs and Patents Act 1988 allows the making of a single copy solely for the purpose of non-commercial research or private study within the limits of fair dealing. The publisher or other rights-holder may allow further reproduction and re-use of this version - refer to the White Rose Research Online record for this item. Where records identify the publisher as the copyright holder, users can verify any specific terms of use on the publisher's website.

Takedown

If you consider content in White Rose Research Online to be in breach of UK law, please notify us by emailing eprints@whiterose.ac.uk including the URL of the record and the reason for the withdrawal request.



eprints@whiterose.ac.uk
<https://eprints.whiterose.ac.uk/>

Supplemental Data

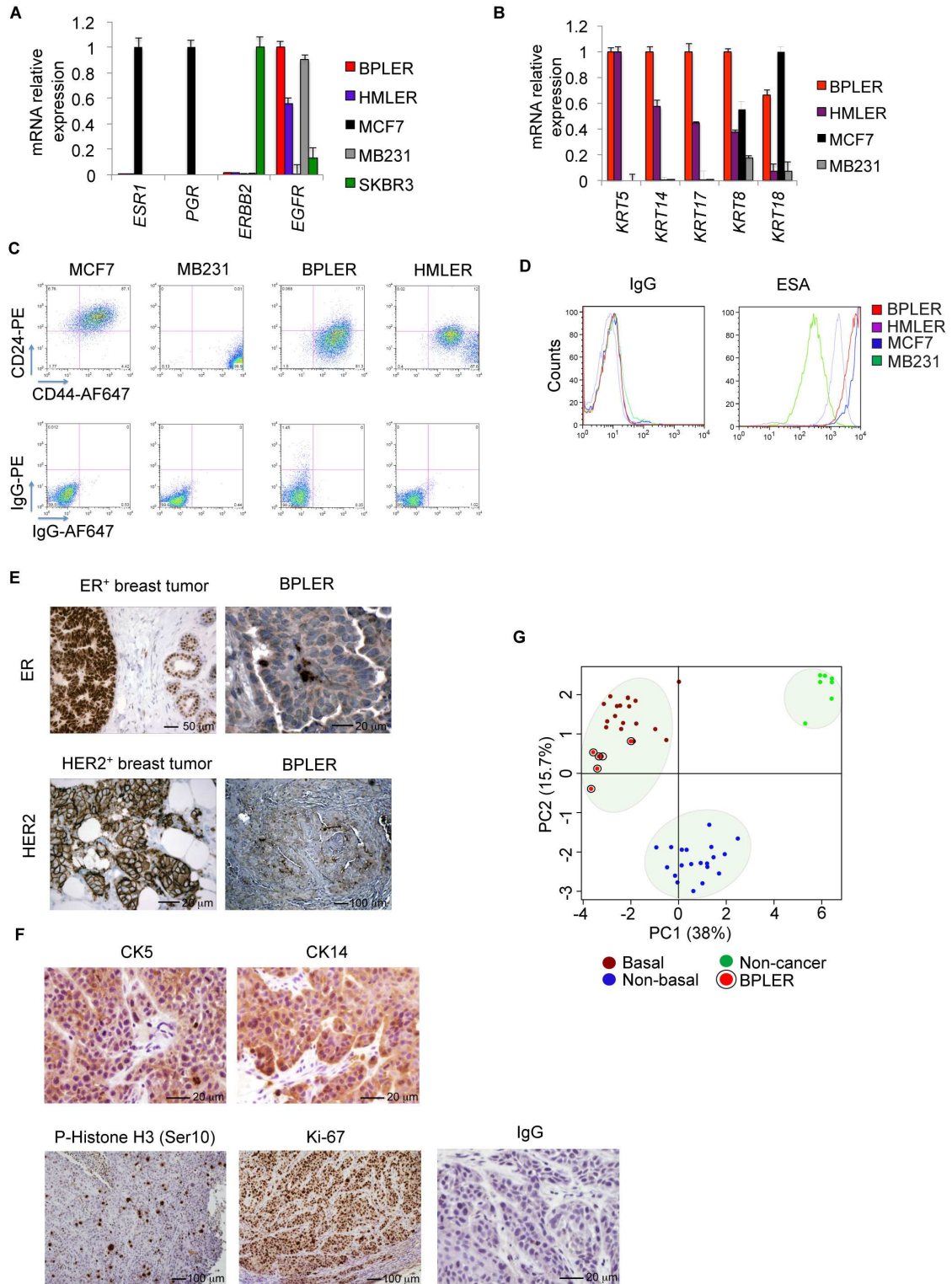


Figure S1, related to Figure 1. BPLER express epithelial breast tumor-initiating cell markers, have an epithelial progenitor cell phenotype and form tumors that resemble basal-like TNBC.

(A) Expression of TNBC markers and *EGFR* mRNA by qRT-PCR in BPLER and HMLER. Luminal MCF7, mesenchymal MB231 and HER2⁺ SKBR3 cells were used as controls.

(B) qRT-PCR quantification of cytokeratin (*CK*) mRNA in BPLER and HMLER cells.

MCF7 and MB231 cells were used as controls. **(C,D)** CD44 and CD24 **(C)** and ESA (EpCAM) **(D)** staining of BPLER and HMLER cells as assessed by flow cytometry.

Luminal MCF7 and mesenchymal MB231 were used as controls. **(E,F)** Representative immunohistochemical staining of BPLER tumors formed after subcutaneous implantation in a nude mouse. ER⁺ and HER2⁺ human breast tumors were used as control. **(G)**

Principal component analysis combining mRNA expression profiles of 6 BPLER tumors grown in immunodeficient mice, 40 human breast primary tumors (classified as either basal-like or non-basal-like) and 7 normal breast tissues (non-cancer) from the Richardson dataset, based on genes that discriminate between the Richardson subtypes.

The two first components are plotted with the proportion of variance explained by each component contained in the axis labels. Data in **(A,B)** were normalized to β -actin mRNA and then to the highest value in the cells tested and represent the mean \pm SD of 3 replicates. All data are representative of at least 3 independent experiments.

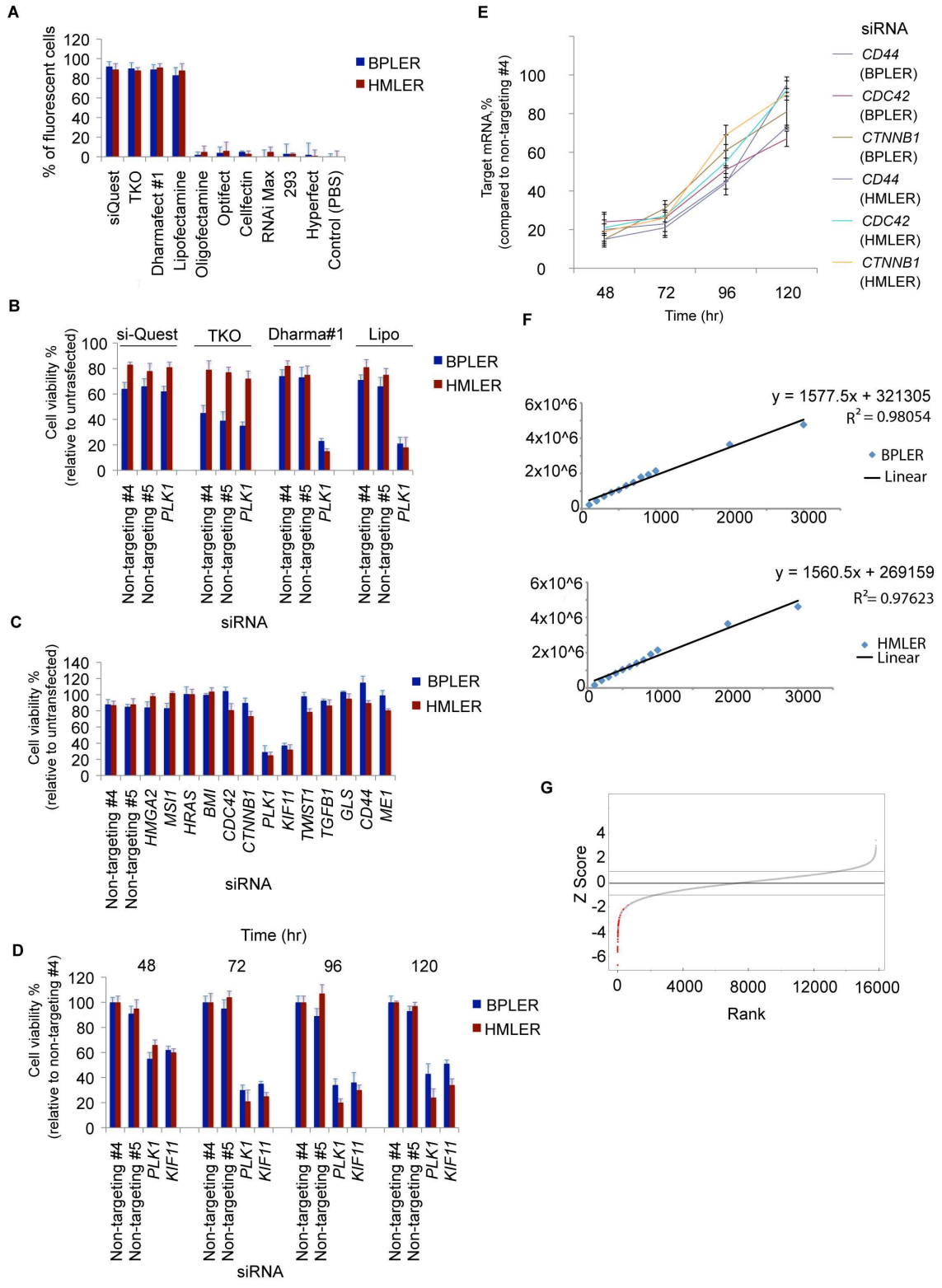


Figure S2, related to Figure 2. siRNA screen optimization.

(A) The reverse-transfection efficiency of BPLER and HMLER cells in WIT medium in 384-well standard tissue culture plates was assessed by flow cytometry using 12 commercially available liposomal formulations complexed with Cy3-labeled siRNAs. Four transfection reagents were able to introduce Cy3-labeled siRNAs into both cell lines with ~90% efficiency. **(B)** Only Dharmafect #1 (Dharmacon) and Lipofectamine 2000 (Invitrogen) had acceptable toxicity (<25% decrease in cell viability) when delivering control non-targeting siRNAs and induced cytotoxicity after transfection with a cytotoxic siRNA targeting *PLK1*. Titration of Dharmafect #1 reduced toxicity in both cell lines to <15% without loss of transfection efficiency (data not shown). Thus Dharmafect #1 was chosen for the screen and used in all subsequent experiments. **(C)** Using Dharmafect #1, 13 pools of siRNAs from the Dharmacon library were transfected in both cell lines to identify additional positive controls besides *PLK1*. **(D)** The optimal time for assessing cell viability was evaluated by assessing viability at indicated times after transfection. **(E)** Durability of gene knockdown in BPLER/HMLER cells, transfected with 3 different non-cytotoxic siRNAs and assessed by qRT-PCR analysis of mRNA expression. Based on data in **(D,E)**, 72 hr was chosen as the optimal time to perform the viability assay for the screen. Values in **A-E** represent the mean \pm SD of three replicates. **(F)** To determine the optimal cell density for the screen, a CellTiterGlo viability assay of BPLER (upper) and HMLER (lower) cells plated for 24 hr at the indicated cell numbers in 384-well plates. Cells were plated at 1000 cells/well for all screening experiments (primary and secondary screens). All data in **(A-F)** are representative of at least three independent experiments. **(G)** Ranked BPLER Z score values for all 17,378 genes represented in the siRNA primary screen library. A Z score with $|Z|>1$ is significant (dotted lines). We required hits to score with $Z_{\leq}-1.5$. Red indicates hits.

Table S1, related to Figure 2. siRNAs that decrease both BPLER and HMLER viability. Provided as an Excel file.

Table S2, related to Figure 2. siRNAs that selectively decrease BPLER viability compared to HMLER. Provided as an Excel file.

Table S3, related to Figure 3. Validated siRNAs that selectively decrease BPLER viability grouped by function. Provided as an Excel file.

Table S4, related to Figure 3. Overlapping annotations between siRNAs that selectively decrease BPLER viability. Provided as an Excel file.

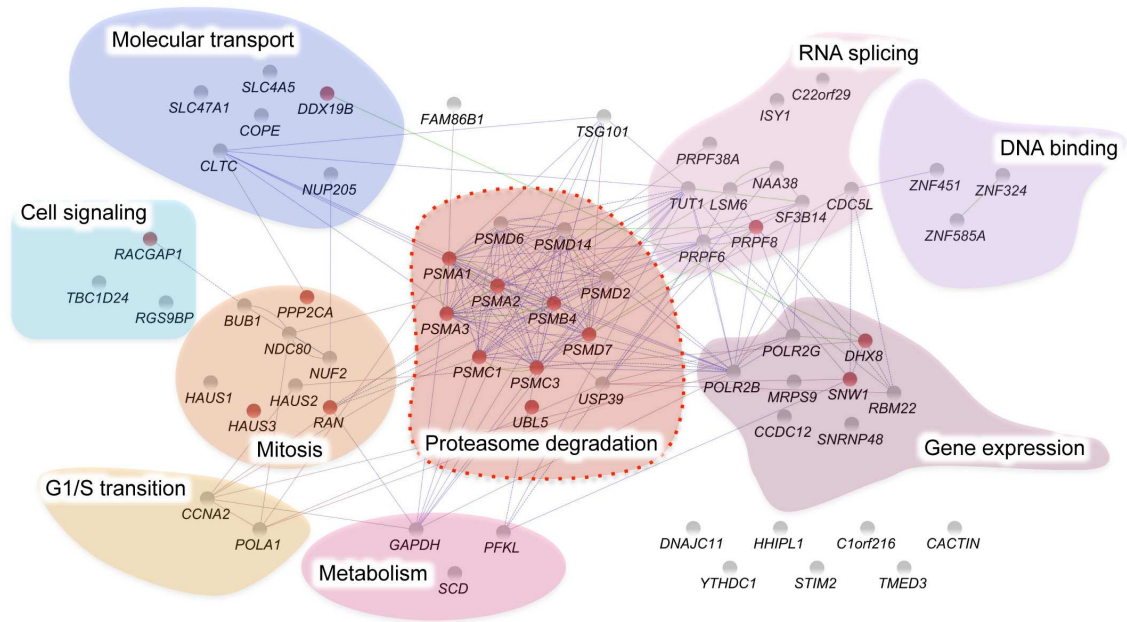


Figure S3, related to Figure 3. Functional analysis of screening hits scoring with at least 2 siRNAs.

The functional/protein interaction network analysis shown in Figure 3 was repeated by restricting the analysis to hits validated with at least 2 of 4 individual siRNAs in the secondary screen.

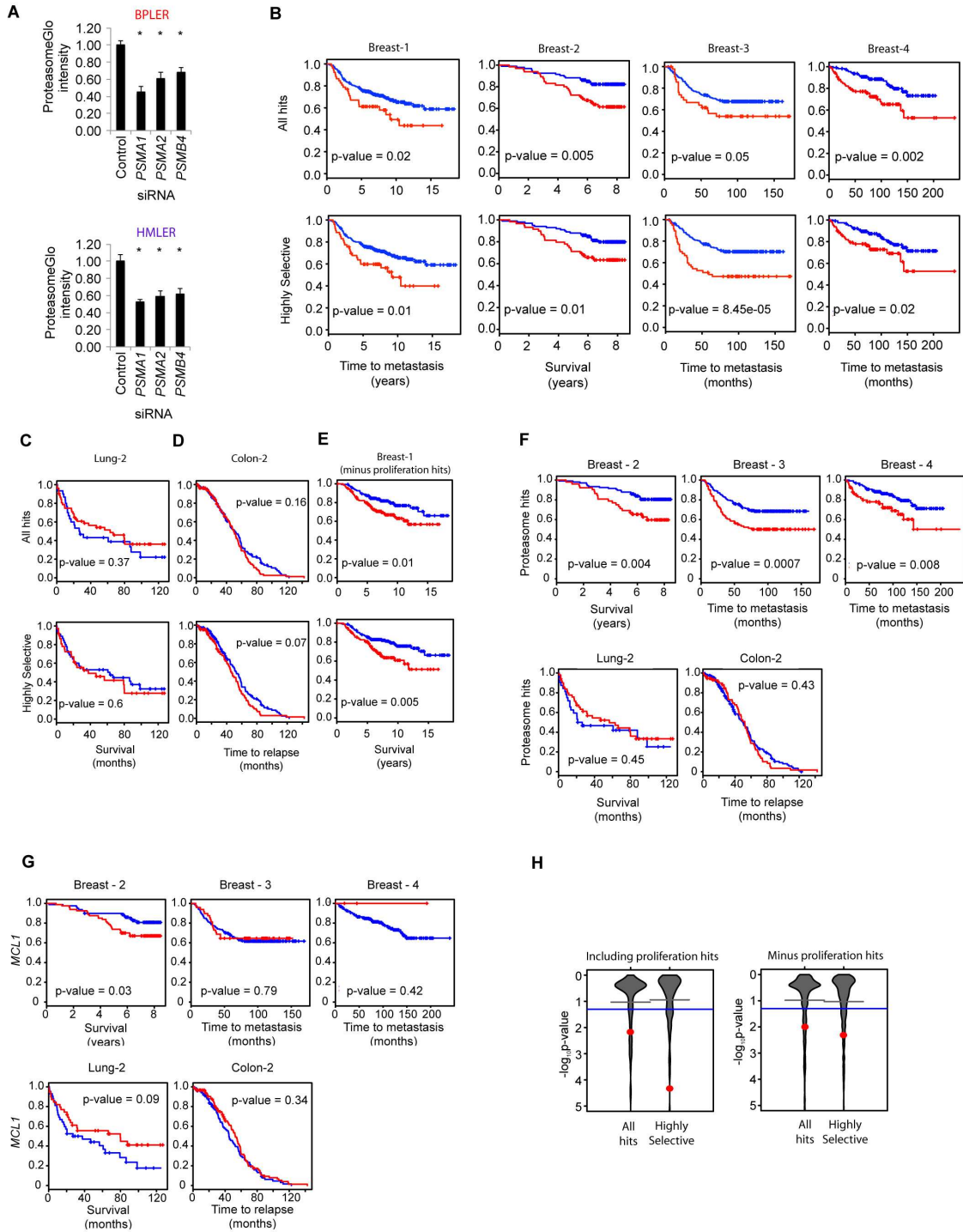


Figure S4, related to Figure 4. Expression of BPLER dependency genes is significantly associated with poor prognosis in breast cancer patients.

(A) Proteasome activity was measured in BPLER and HMLER by Proteasome-Glo assay 72 hr after transfection with a non-targeting siRNA (control) or siRNA pools against catalytic (*PSMB4*) or non-catalytic (*PSMA1*, *PSMA2*) proteasome subunits in the proteasome modules in Figure 3 and S3. For BPLER, zVAD-fmk (20 μ M) was added to prevent apoptosis caused by proteasome inhibition. Proteasome activity was normalized to the number of viable cells after 72 hr. Data shown are mean \pm SD of 3 experiments. *, $p < 0.05$. **(B-D)** Kaplan-Meier (K-M) curves depicting overall or metastasis-free survival for breast **(B)**, lung **(C)** and colon **(D)** cancer patients in independent datasets (Table S5) based on tumor expression of all BPLER dependency genes (top row) or the highly selective subset (bottom row). Patients from each dataset were divided into two groups based on their tumor's GSEA enrichment score. The high expressing tumors (red) were defined by enrichment scores with p -value < 0.1 , and the remaining tumors were classified as low (blue). **(E)** Correlation of both all the hits (top) and the subset of highly selective hits (bottom) with prognosis in breast cancer after elimination of proliferation-related genes, as defined in (Venet et al., 2011). **(F-G)** K-M curves depicting overall or metastasis-free survival for breast, lung and colon cancer patients in independent datasets (Table S5) based on tumor expression of **(F)** proteasome-related hits (Figure 3) or **(G)** *MCL1*. **(H)** P-value of K-M estimator of patients in the NKI dataset stratified by expression of all hits or the highly selective hits (left), and the same gene sets with proliferation-associated genes removed (right). The red dot indicates the K-M p-value, and the grey cone is a bean plot representing the distribution of p-values from 1000 randomly selected gene sets of the same size. The blue line indicates a p-value of 0.05.

Table S5, related to Figure 4. Tumor datasets used for Figures 4 and S4.

Dataset	Outcome Event	n	Events	ER⁺ (n)	ER⁻ (n)	% ER neg	GEO	Reference
Breast_1	Overall Survival	295	78	226	69	23	-	van de Vijver et al., 2002
Breast_2	Overall Survival	159	46	130	29	18	GSE1456	Pawitan et al., 2005
Breast_3	Metastasis-free Survival	286	107	209	77	27	GSE2034	Wang et al., 2005
Breast_4	Metastasis-free Survival	200	28	156	44	22	GSE11121	Schmidt et al., 2008
Lung_1	Overall Survival	111	58	-	-	-	GSE3141	Bild et al, 2006
Lung_2	Overall Survival	82	50	-	-	-	GSE19188	Hou et al, 2010
Colon_1	Overall Survival	232	93	-	-	-	GSE17538	Smith et al, 2010
Colon_2	Relapse	226	177	-	-	-	GSE14333	Jorissen et al, 2009

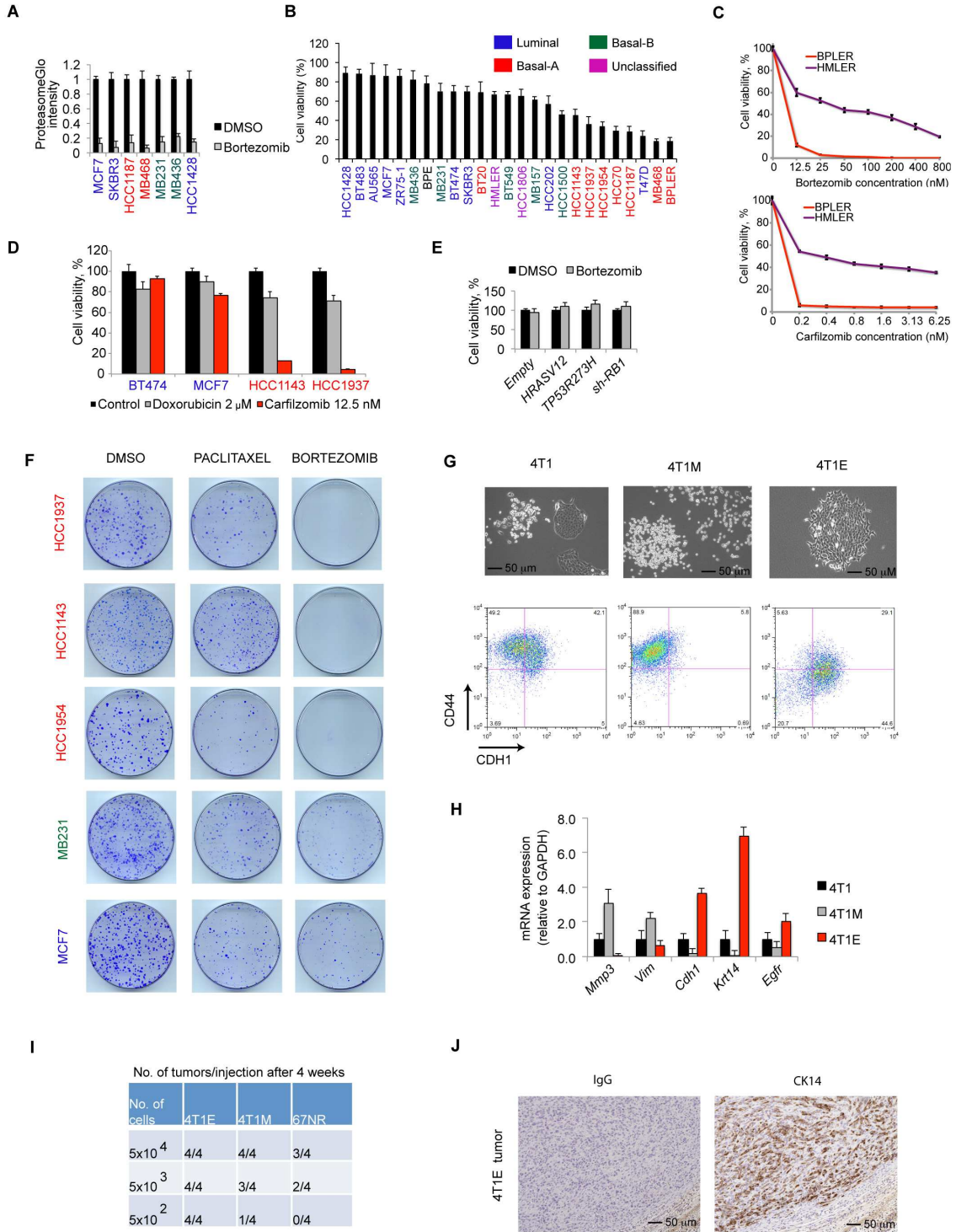


Figure S5, related to Figure 5. Effect of proteasome inhibitor drugs on breast cancer cell lines.

(A) Proteasome activity as measured by Proteasome-Glo assay in breast cancer cell lines 8 hr following treatment with bortezomib (12.5 nM) or DMSO, at a time when most cells are viable (not shown). **(B)** Viability of a panel of 25 cell lines of different subtypes treated for 24 hr with bortezomib (12.5 nM) relative to vehicle control, as assessed by CellTiter-Glo. **(C)** Dose-response curve of BPLER and HMLER treated with bortezomib (top) or carfilzomib (bottom) at the indicated concentrations for 24 hr. **(D)** Viability of breast cancer cell lines treated with carfilzomib (12.5 nM) for 24 hr. **(E)** Viability of MCF7 cells 24 hr after treatment with bortezomib (12.5 nM) or DMSO. Cells were transduced with a pBABE retroviral vector carrying *HRAS*^{V12}, *TP53R273H* (a dominant mutant of *TP53*) or an shRNA against *RB1* (or empty vector) and selected with puromycin (2 μ M) for 4 weeks. These cell lines retain a luminal phenotype and display ~ 8-fold up-regulation of mutant *HRAS* and *TP53* and ~10-fold down-regulation of *RB1* compared to parental MCF7 cells, as determined by qRT-PCR (not shown). **(F)** Colony assays of breast cancer cell lines treated with bortezomib (12.5 nM) or paclitaxel (100 nM) for 18 hr and cultured for 8 days in drug-free medium. **(G)** At least 2 cell types with distinct morphology can be identified in 4T1 after plating at clonal density. These cells, which we termed 4T1E (epithelial) and 4T1M (mesenchymal), can be separated by FACS based on surface expression of CD44 and E-cadherin (CDH1). **(H)** qRT-PCR analysis showing differential expression of epithelial vs. mesenchymal markers in 4T1E vs. 4T1M. **(I)** Incidence of breast primary tumors 4 weeks after injection of indicated numbers of 4T1E and 4T1M cells in the mammary fat-pad of BALB/c mice. 67NR, a mouse breast cancer cell line derived from the same parental tumor as 4T1, was used as control. **(J)** 4T1E tumors stain for the basal-like marker CK14 by immunohistochemistry. Data shown in **(A-E,H)** are mean +/- SD of at least 3 experiments.

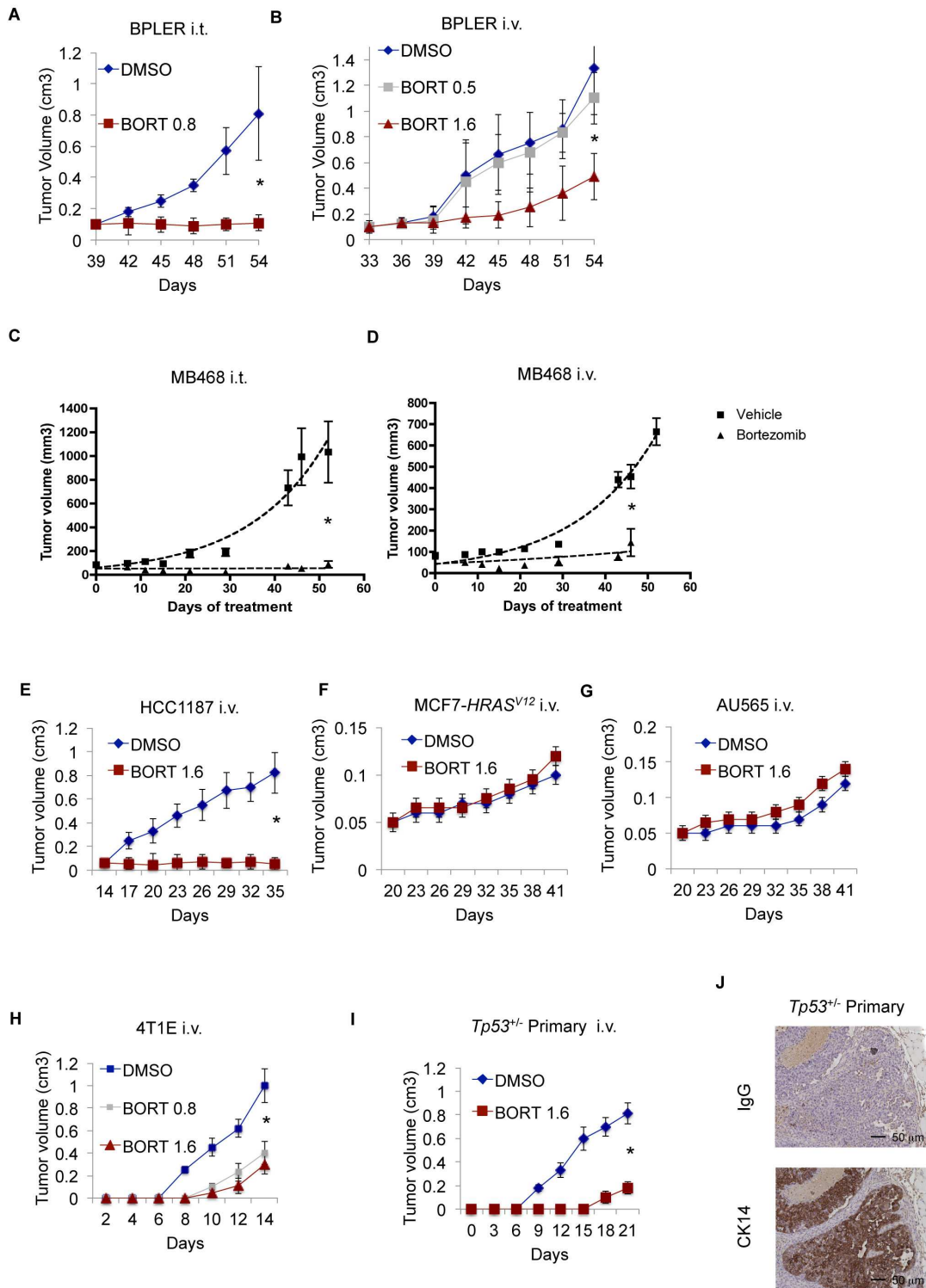


Figure S6, related to Figure 6. Bortezomib suppresses TNBC growth in vivo.

(A-E) Mean tumor volume +/- SD in BPLER **(A,B)**, MB468 **(C,D)**, HCC1187 **(E)**, MCF7-*HRAS*^{V12} **(F)**, AU565 **(G)** and 4T1E **(H)** tumor-bearing mice after bortezomib (BORT) treatment at the indicated dose and route of administration. Bortezomib was given weekly (i.v.) or q3d (i.t.). DMSO was administered to control mice (N=8 mice/group in **(A-D,H)**; N=5 mice/group in **(E-G)**). Treatments were started when tumors became palpable (~50-100 mm³). **(I)** Mean tumor volume +/- SD in BALB/c mice implanted with tumor fragments from a primary mouse tumor spontaneously arising in a *Tp53*^{+/-} BALB/c mouse. Recipient mice were treated with i.v. bortezomib at the indicated dose (or DMSO) starting 2 days after implantation. **(J)** Histological analysis of primary tumor used in **(I)**, showing features of basal-like TNBC, including epithelial differentiation, scant stroma and CK14 staining.

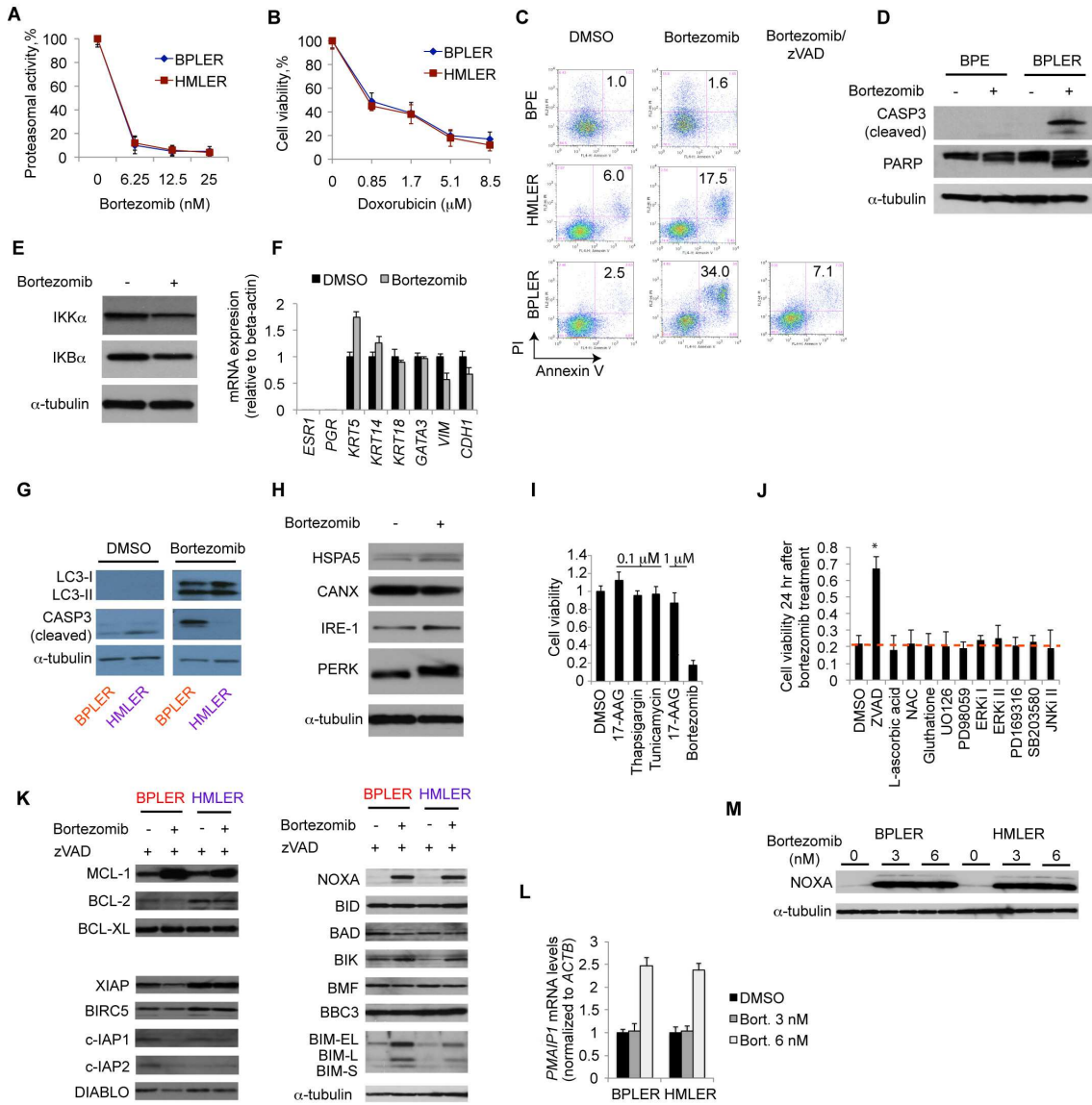
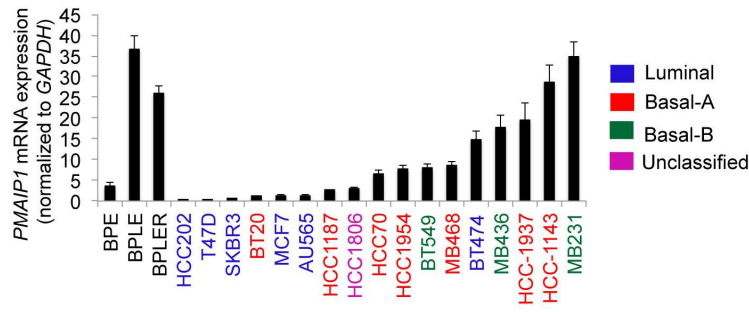


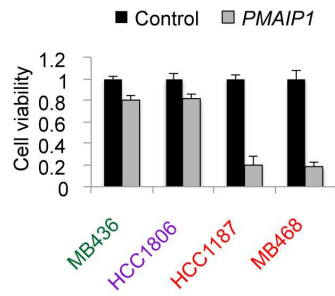
Figure S7, related to Figure 7. Bortezomib promotes apoptosis in BPLER that is independent of effects on NF- κ B signaling, cell differentiation, autophagy, or oxidative or ER stress.

(A) Proteasome activity in BPLER and HMLER 6 hr after treatment with the indicated dose of bortezomib, as determined by ProteasomeGlo assay. At this time most cells are viable (data not shown). **(B)** Viability of BPLER and HMLER cells 24 hr after treatment with the indicated doses of doxorubicin. **(C)** Flow cytometry analysis of Annexin V/Propidium Iodide (PI) staining of BPE, BPLER or HMLER treated with bortezomib (12.5 nM) and/or zVAD-fmk (20 μ M). The percentage of double positive cells is indicated. **(D)** Immunoblot of lysates from BPE and BPLER cells treated with bortezomib (12.5 nM) for 24 hr assessed for caspase and PARP cleavage. **(E-G)** Immunoblot and qRT-PCR analysis of BPLER cells treated with bortezomib or DMSO for 24 hr showing expression levels of NF- κ B signaling regulators **(E)**, epithelial differentiation markers **(F)** and autophagy markers **(G)**. **(H)** Immunoblot for ER stress markers in BPLER 24 hr after bortezomib treatment. **(I)** Cell viability in BPLER cells 24 hr after treatment with three ER stressors at the indicated concentrations relative to DMSO-treated cells. **(J)** Cell viability of bortezomib-treated BPLER cells (12.5 nM for 24 hr) in the presence of antioxidants or inhibitors of MEK, ERK, p38 or JNK. The concentration used for each agent and its target are provided in Supplemental Experimental Procedures. **(K)** Immunoblot of BPLER and HMLER treated with bortezomib or DMSO at the indicated dose for 24 hr in the presence of 20 μ M zVAD-fmk. **(L,M)** *PMAIP1* mRNA **(L)** and NOXA protein **(M)** levels assessed by qRT-PCR and immunoblot, respectively, in BPLER and HMLER treated with bortezomib (Bort.) at the indicated dose for 24 hr. Data in **(A,B,F)** are mean \pm SD of 3 experiments.

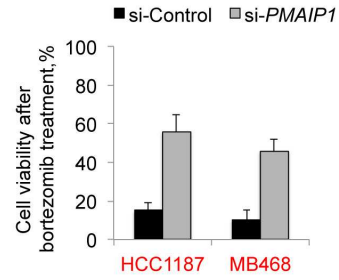
A



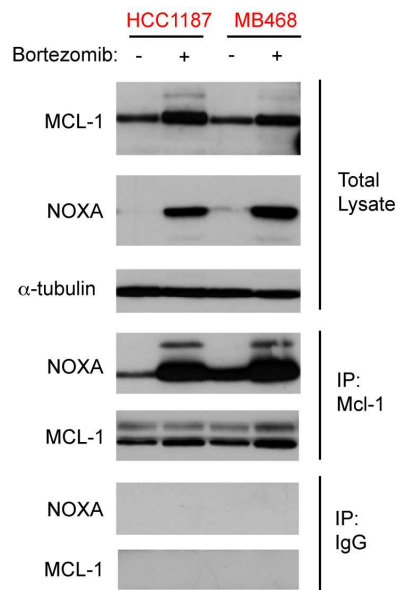
B



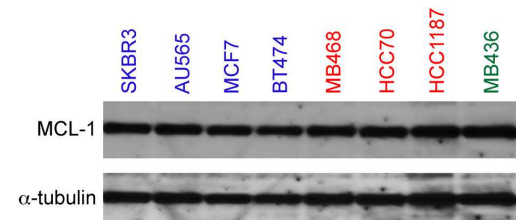
C



D



E



F

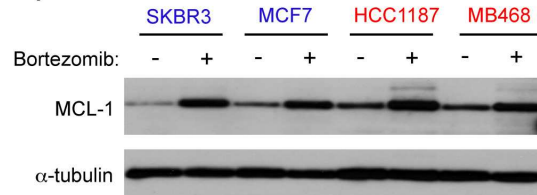


Figure S8, related to Figure 8. NOXA mediates bortezomib cytotoxicity in basal-like cell lines and binds MCL-1.

(A) Baseline levels of *PMAIP1* mRNA, relative to *GAPDH*, by qRT-PCR in normal breast epithelial cells at different stages of transformation (BPE, BPLE, BPLER (Figure 1A)) and in breast cancer cell lines of different subtypes. **(B)** Cell viability in bortezomib-sensitive basal-like (MB468, HCC1187) and bortezomib-resistant non-basal-like (MB436, HCC1806) cell lines 24 hr after transfection with a vector expressing *PMAIP1* ORF or empty vector. **(C)** Viability of basal-like MB468 and HCC1187 cells transfected with a non-targeting siRNA (control) or an siRNA against *PMAIP1*. Viability was measured 24 hr after treatment with bortezomib (12.5 nM) or DMSO that was initiated 24 hr after siRNA transfection. **(D)** Analysis of MCL-1/NOXA binding by immunoprecipitation in bortezomib-sensitive HCC1187 and MB468 18 hr after treatment with bortezomib (12.5 nM) in the presence of zVAD-fmk. **(E,F)** Immunoblot of cell lysates from breast cancer cell lines with varying bortezomib sensitivity under baseline conditions **(E)** and after treatment with bortezomib (12.5 nM) for 24 hr in the presence of zVAD-fmk **(F)**. Data in **(A-C)** are mean +/- SD of 3 experiments.

Supplemental Experimental Procedures

Cell culture. Human BPE, BPLE, BPLER and HMLER cells were grown in WIT medium (Stemgent). All experiments were performed with pairs of cells derived from the same patient (BPLER-2 and HMLER-2). MB468 were transduced with a luciferase reporter and kindly provided by Dr. Andrew Kung. All other human cell lines were obtained from ATCC and grown in MEM (MCF7, BT474, BT20), McCoy's 5A (SKBR3, AU565), RPMI1640 (MB436, MB231, BT549, HCC1806, HCC202, HCC1143, HCC1937, HCC1954, HCC70, HCC1187, MB468, T47D, HCC1428, ZR75-1, BT483) or L15 (MB157) all supplemented with 10% FBS unless otherwise indicated. 4T1 mouse breast cancer cells, a kind gift of Dr. Fred Miller, were grown in 10% FBS DMEM. 4T1E cells were purified from the bulk of 4T1 cells by fluorescence activated cell sorting based on positive E-cadherin expression. 4T1E cells display an epithelial phenotype, are triple-negative, express basal-like TNBC markers CK5/CK14 and murine T-IC markers CD49f and CD24, and give rise to tumors in BALB/c mice with as few as 5,000 cells (Fig. S5 and data not shown). For screening and functional experiments cells were reverse-transfected with pools of 4 different siRNAs targeting distinct regions within the same gene (50 nM) using Dharmafect#1 (Dharmacon) in WIT medium (BPLER, HMLER) or Opti-MEM (all other cell lines). Medium was replaced with fresh WIT medium after 24 hr. Scrambled siRNAs (siRNA control #4 or #5, Dharmacon) were used as controls. Both control siRNAs were not cytotoxic. Gene silencing (>70%) was verified by qRT-PCR for all functional experiments. For drug treatment, cells were plated at low density (30,000-80,000 cells/well in 6-well plates or 1000 cells/well in 384-well plates) and treated either immediately or 24 hr later. Bortezomib treatment of transfected cells was begun 24 hr after transfection. In each case, cells were not allowed to reach confluence. All drug treatments were performed in WIT medium, since the effect of bortezomib on

proteasome activity was reduced in 10% FBS DMEM (not shown). Cell viability was assessed by CellTiter-Glo (Promega) in 384-well plates or by Trypan-Blue staining in 6-well plates. Proteasome activity was assessed by Proteasome-Glo (Promega) in 384-well plates. Chemoluminescence was measured using an Envision (PerkinElmer) high-throughput plate reader. Selective sensitivity to proteasome inhibition was most evident after treatment with clinically relevant doses of bortezomib (12.5 nM) for 18-24 hr. As expected, after prolonged inhibition of proteasome function (>24-36 hr), all cells showed signs of toxicity. For colony formation assay, 1,000 viable cells were plated on 10-cm plates in serum-containing medium. Medium was replaced every 3 d. After 8-14 d, cells were fixed in methanol (-20 °C) and stained with crystal violet. For sphere formation assay, 1,000/ml viable cells were cultured in suspension in serum-free DMEM/F12 1:1 (Invitrogen), supplemented with EGF (20 ng/ml, BD Biosciences), B27 (1:50, Invitrogen), 0.4% bovine serum albumin (Sigma) and 4 µg/ml insulin (Sigma). Spheres were counted after 1 or 2 weeks.

siRNAs used in this study:

siRNA	Catalog #	Source
<i>BAD</i>	M-003870-02	Dharmacon
<i>BAK</i>	M-003305-02	Dharmacon
<i>BAX</i>	M-003308-03	Dharmacon
<i>BCL2</i>	M-003307-06	Dharmacon
<i>BCL2L1</i>	M-003458-06	Dharmacon
<i>BID</i>	M-004387-02	Dharmacon
<i>BIK</i>	M-004388-02	Dharmacon
<i>BIM</i>	6518	Cell Signaling
<i>BIRC5</i>	M-003459-03	Dharmacon
<i>BMF</i>	M-004393-04	Dharmacon
<i>BOK</i>	M-004394-00	Dharmacon
<i>BUB1</i>	M-004102-01	Dharmacon
<i>CASC5</i>	M-015673-01	Dharmacon
<i>CASP8</i>	M-003466-05	Dharmacon
<i>CDK1</i>	M-003224-03	Dharmacon
<i>CDK5</i>	M-003239-01	Dharmacon
<i>DDX19B</i>	M-013471-01	Dharmacon
<i>DHRS13</i>	M-008777-01	Dharmacon
<i>FADD</i>	M-003800-03	Dharmacon
<i>FAS</i>	M-003776-04	Dharmacon
<i>GAPDH</i>	M-004253-02	Dharmacon
<i>HRAS</i>	M-004142-00	Dharmacon
<i>MCL1</i>	M-004501-08	Dharmacon
<i>NDC80</i>	M-004106-00	Dharmacon
<i>NFKB1</i>	M-003520-01	Dharmacon
<i>NUF2</i>	M-005289-02	Dharmacon
<i>TP53</i>	M-003329-03	Dharmacon
<i>TP63</i>	M-003330-01	Dharmacon
<i>TP73</i>	M-003331-01	Dharmacon
<i>PFKL</i>	M-006822-00	Dharmacon
<i>PMAIP1</i>	M-005275-03	Dharmacon
<i>PRPF8</i>	M-01225202	Dharmacon
<i>PSMA1</i>	M-010123-01	Dharmacon
<i>PSMA2</i>	M-011757-01	Dharmacon
<i>PSMB4</i>	M-011362-00	Dharmacon
<i>PUMA</i>	M-004380-01	Dharmacon
<i>RAN</i>	M-010353-00	Dharmacon
<i>RELA</i>	M-003533-02	Dharmacon
<i>RFT1</i>	M-018174-00	Dharmacon
<i>SPRY2</i>	M-005206-01	Dharmacon

<i>TNF</i>	M-010546-01	Dharmacon
<i>TNFRSF1B</i>	M-003934-00	Dharmacon
<i>TNFRSF10A</i>	M-008090-02	Dharmacon
<i>TNFRSF10B</i>	M-004448-00	Dharmacon
<i>XIAP</i>	M-004098-01	Dharmacon

Small molecules used in Figure S7J:

Chemical	Final concentration	Target	Source
zVAD-fmk	20 μ M	Caspases	BDBiosciences
ERKi I	20 μ M	ERK	EMD
ERKi II	5 μ M	ERK	EMD
UO126	10 μ M	MEK	Sigma
PD98059	10 μ M	MEK	Sigma
JNKi II	100 nM	JNK	EMD
PD169316	10 μ M	p38	EMD
SB203580	20 μ M	p38	Sigma
NAC	200 μ M	Oxid. Stress	Sigma
Glutathione	200 μ M	Oxid. Stress	Sigma
L-ascorbic acid	100 μ M	Oxid. Stress	Sigma
Bortezomib	12.5 nM	Proteasome	LC Laboratories

RNA analysis. qRT-PCR analysis was performed as described (Petrocca et al., 2008). Briefly, total RNA was extracted with Trizol (Invitrogen) and cDNA prepared from 600-900 ng total RNA using Thermoscript RT kit (Invitrogen) as per the manufacturer's instructions. 2.5 ml of diluted cDNA (1:20) was used as template for qPCR using Power SYBR Green Master Mix (Applied Biosystems) and a Biorad C1000 Thermal Cycler (Biorad). Primer sequences are available upon request. Relative CT values were normalized to β -actin and converted to a linear scale using the $-\Delta$ CT method.

Protein analysis. Immunoblot was performed as described (Petrocca et al., 2008). Primary antibodies were as follows: cleaved CASP3 (Cell Signaling, rabbit polyclonal,

1:1000), PARP (Santa Cruz, rabbit polyclonal, 1:500), MCL-1 (Cell Signaling, Rabbit polyclonal, 1:1000), BIM (Santa Cruz, rabbit polyclonal, 1:500), BIK (Cell Signaling, rabbit polyclonal, 1:1000), PUMA (Cell Signaling, rabbit polyclonal, 1:1000), NOXA (Calbiochem, mouse monoclonal, 1:500), BID (Santa Cruz, rabbit polyclonal, 1:500), BAD (Santa Cruz, rabbit polyclonal, 1:500), BCL-2 (Santa Cruz, rabbit polyclonal, 1:500), BCL-XL (Cell Signaling, 1:000, rabbit polyclonal), XIAP (Cell Signaling, 1:000, rabbit polyclonal), Survivin (Cell Signaling, 1:000, rabbit polyclonal), c-IAP1 (Cell Signaling, 1:000, rabbit polyclonal), c-IAP2 (Cell Signaling, 1:000, rabbit polyclonal), DIABLO (Cell Signaling, 1:000, rabbit polyclonal), BMF (Cell Signaling, 1:000, rabbit polyclonal), IKK α (Cell Signaling, 1:1000, rabbit), IKB α (Cell Signaling, 1:1000, rabbit), HSPA5, CALX, IRE-1 and PERK (ER stress kit, Cell Signaling, Rabbit, 1:1000). Antibodies were diluted in 5% milk in TBS-Tween and incubated overnight at 4°C. Secondary mouse and rabbit HRP-conjugated antibodies were from Amersham. Protein signal was detected using the ECL Plus kit (Amersham). Dynabeads Protein G (Invitrogen) and magnetic separation were used for immunoprecipitation studies, according to the manufacturer's instructions. For immunofluorescence microscopy, cells were fixed in 2% formaldehyde for 10 min, permeabilized with 1% Triton X in PBS for 5 min, and incubated with primary antibodies in 0.5% Triton X, 1% FBS in PBS for 30 min at RT. Antibodies were: CK18 (Santa Cruz, mouse monoclonal, 1:100) and CK14 (Millipore, mouse monoclonal, 1:100). After washing the cells were stained sequentially with AlexaFluor-647-conjugated secondary antibody (Invitrogen, 1:200) and DAPI (Sigma, 1:5000). For immunohistochemistry, tumor sections were prepared from paraffin-embedded tissues, deparaffinized and treated with 10% citrate buffer for 15 min. Staining was performed using a Biogenex IHC DAB kit (Biogenex) following the manufacturer's protocol. Primary antibodies were: CK14 (Millipore, mouse monoclonal, 1:100), CK5 (Millipore, mouse monoclonal, 1:100),

phospho-Histone H3 (Ser10) (Cell Signaling, rabbit polyclonal, 1:100), vimentin (Invitrogen, mouse monoclonal 1:100), Ki67 (Millipore, mouse monoclonal, 1:100).

Flow cytometry. For flow cytometry, cells were stained as previously described (Yu et al., 2007), using the following fluorescent-conjugated antibodies: CD44 (BD Biosciences), CD24 (BD Biosciences), CD326 (ESA, Biolegend). For cell-cycle analysis, cells were fixed in cold methanol, RNase-treated, and stained with propidium iodide (Sigma). Cells were analyzed for DNA content by FACSCalibur (BD Biosciences) by using doublet discrimination gating. All analyses were performed in triplicate and 20,000 gated events/sample were counted. For apoptosis analysis, cells were washed in cold PBS, incubated with Annexin V-APC (Invitrogen) and PI (Sigma) for 15 min in the dark, and analyzed within 1 hr. Mitochondrial membrane depolarization was measured by Mitoprobe DiIC1(5) assay (Invitrogen), according to the manufacturer's instructions.

Screening hit selection. Viability scores were judged based on a combination of parameters, including relative standard deviation among replicates (RSD), median absolute deviation (MAD)-based Z score (Z score), fold-change from the plate median (FC), and BPLER/HMLER FC ratio (R) (Birmingham et al., 2009). For each set of triplicate plates, siRNAs with RSD >0.25 were excluded. Any siRNAs causing severe cytotoxicity to HMLER (HMLER Z score \leq -3 or HMLER FC \leq 0.5) were also excluded from further analysis. siRNAs were considered hits if they satisfied the following criteria: BPLER Z score \leq -1.5, BPLER FC \leq 0.75, R \leq 0.75. Positive hits were classified into highly, moderately or modestly selective based on R values. The positive hits were subjected to a secondary screen in which cells were transfected individually with the 4 siRNAs in the positive pools. Hits were considered validated if wells treated with at least

one siRNA in the pool met the same criteria used in the primary screen, since many siRNA pools may have only 1 effective siRNA.

Survival and metastasis-free survival analysis of primary tumor datasets. The prognostic power of the 154 gene signature and the 23 most highly selective confirmed hits was evaluated before and after removal of the genes in the meta-PCNA proliferation gene list of (Venet et al., 2011) corresponding to the 1% of genes most positively correlated with proliferation marker PCNA in a compendium of normal tissue expression. For each of the clinical datasets, samples were stratified into 2 groups based on the summed median-zeroed expression Z-score of the signature genes. Survival curves and p-value estimates were calculated using the Kaplan-Meier method using the survival package in R. The analysis was repeated using 1000 random signatures of identical size as the test signatures to build a background of p-values.

Comparing the expression of the BPLER dependency genes across cancer subtypes. A score for the expression of the 154 gene signature and the 23 most highly selective was calculated across each of the 295 human breast primary cancers in the NKI database by the mean-ranked expression of the genes within the gene sets, using the single chip enrichment script within the pathprint package. A Z-score for the gene set expression was calculated using the scores from all the samples, and plotted as bean-plots to compare the distribution of the gene signature expression in each of the different tumor subtypes (Basal, basal-like; Lum, luminal; NL, normal-like). Each bean consists of a green line for each sample with the overall distribution represented as a gray density shape and a black line indicating the median Z score.

In vivo experiments. Exponentially growing tumor cells were trypsinized with Tryple Express (Invitrogen), resuspended in a 1:1 WIT-Matrigel solution at the indicated numbers, and injected subcutaneously in the flank of 4-week old female Nu/J mice (Stock # 002019, Jackson Laboratories). For proteasome inhibition studies in vivo, bortezomib was first dissolved in DMSO (10 mM) and then diluted in PBS to the indicated concentration. Tumor-bearing mice were treated with 0.8 mg/kg bortezomib in PBS intratumorally (50 μ l), intraperitoneally (100 μ l) or intravenously (100 μ l), or 1.6 mg/kg bortezomib in PBS intravenously (100 μ l). After 18 hr, mice were sacrificed and tumors lysed. Proteasome activity was measured by Proteasome-Glo assay (Promega), according to the manufacturer's protocol. For bortezomib treatment of human tumor xenografts, beginning ~33 d after cells were injected (when tumors became palpable), mice bearing tumors of comparable size were randomized into two groups and treated with bortezomib or DMSO, respectively, at the indicated dose. For 4T1E experiments, 2×10^5 cells in PBS were injected in the mammary fatpad or tail vein of syngeneic BALB/c mice. Bortezomib treatment was started 2 days after injection. Lung metastatic nodules were visualized by India ink injected intratracheally after mice were sacrificed. For experiments on primary tumor fragments, breast tumors arising in *Tp53*^{+/-} BALB/c mice were resected and fragments implanted in the mammary fat-pad of recipient WT BALB/c mice. Bortezomib treatments were started 2 days after implantation. For tumor initiation experiments, 4T1E cells, treated with bortezomib (12.5 nM) or DMSO in vitro for 18 hr, were injected in the mammary fatpad of BALB/c mice using 50,000 cells and tumor growth was monitored for 30 days. For all experiments, tumor diameters were measured every 2-3 days, and tumors were weighed after necropsy. Tumor volumes were calculated by using the equation $V = a \times b^2/2$, where a is the largest diameter and b is the perpendicular diameter.

Supplemental References

Birmingham, A., Selfors, L. M., Forster, T., Wrobel, D., Kennedy, C. J., Shanks, E., Santoyo-Lopez, J., Dunican, D. J., Long, A., Kelleher, D., *et al.* (2009). Statistical methods for analysis of high-throughput RNA interference screens. *Nat Methods* 6, 569-575.

Petrocca, F., *et al.* (2008). E2F1-regulated microRNAs impair TGFbeta-dependent cell-cycle arrest and apoptosis in gastric cancer. *Cancer Cell* 13, 272-286.

Yu, F. *et al.* (2007). let-7 Regulates Self Renewal and Tumorigenicity of Breast Cancer Cells. *Cell* 131, 1109-1123.